WEATHER CLIMATE WATER

WORLD METEOROLOGICAL ORGANIZATION

GLOBAL ATMOSPHERE WATCH

WMO GREENHOUSE GAS BULLETIN

The State of Greenhouse Gases in the Atmosphere
Based on Global Observations through 2018

No. 15 | 25 November 2019

ISSN 2078-0796

Isotopes confirm the dominant role of fossil fuel combustion in increasing levels of atmospheric carbon dioxide

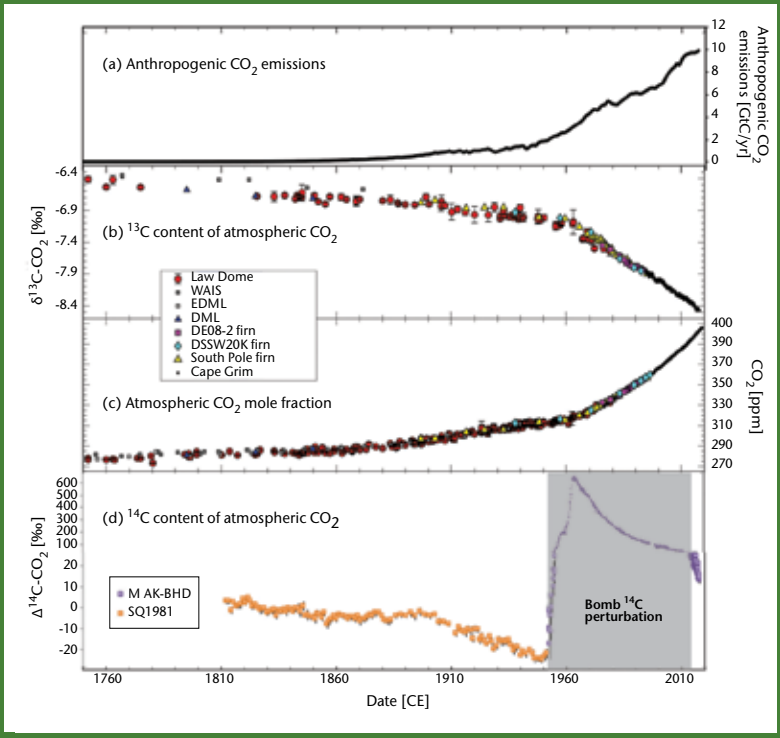

Measurements of the content of radiocarbon (^{14}C) in atmospheric carbon dioxide (CO_2) provide a unique way to discriminate between fossil fuel combustion and natural sources of CO_2. Simultaneous observations of CO_2 and ^{14}C demonstrate the decline of ^{14}C content in atmospheric CO_2 caused by CO_2 addition from fossil fuel combustion. This finding illustrates the importance of long-term measurements of atmospheric composition by laboratories involved in the WMO Global Atmosphere Watch (GAW) Programme in helping identify greenhouse gas emission sources.

Three isotopes of carbon are found in natural systems: ^{12}C (~99% of all carbon), ^{13}C (~1%) and ^{14}C (~1 part per trillion). All carbon isotopes are present throughout the carbon cycle, but the relative proportion of each isotope in different carbon reservoirs varies, providing unique "fingerprints" for each reservoir. Therefore, measuring the isotopic composition of atmospheric CO_2 helps identify and quantify its sources and sinks.

$^{14}CO_2$ is produced in very small amounts in the upper atmosphere by cosmic rays. ^{14}C is radioactive and decays slowly with a half-life of 5 700 years, resulting in a small but measurable ^{14}C content in atmospheric CO_2 and in plant materials formed from CO_2. Fossil fuels were formed from plant material millions of years ago, hence any ^{14}C present when the plants were alive has since decayed during their stay in the Earth's crust.

^{13}C is a stable isotope, meaning that the ^{13}C content of fossil fuels does not change over time. However, the plants from which fossil fuels were formed take up ^{12}C in preference to ^{13}C, so that fossil fuels contain less ^{13}C than the current atmospheric CO_2. Fossil fuel combustion, therefore, also results in a decline in the ^{13}C content of atmospheric CO_2.

The figure on the left shows the development of CO_2 emissions (panel a) [1, 2], atmospheric abundance (b) and isotope ratios (c) of CO_2, since 1760, from air trapped in ice cores and air collected at Cape Grim, Australia [3], and ^{14}C content (d) of atmospheric CO_2 from tree rings [4, 5] and air collected at Wellington, New Zealand [6]. As anthropogenic emissions have increased, atmospheric CO_2 has increased also. At the same time, both the ^{13}C and ^{14}C content of atmospheric CO_2 have declined, as the fossil fuel CO_2 emitted into the atmosphere has no ^{14}C and a lower ^{13}C content than the current atmosphere. The simultaneous decline in both ^{13}C and ^{14}C content alongside CO_2 increases can only be explained by the ongoing release of CO_2 from fossil fuel burning.

The ^{14}C fossil fuel signal in atmospheric CO_2 was swamped by the near doubling of ^{14}C in the atmosphere in the early 1960s due to ^{14}C produced by atmospheric nuclear weapons testing (see panel (d) in the figure on the left), making ^{14}C unusable for fossil fuel detection since the early 1950s. Yet that human-produced ^{14}C spike has now roughly levelled throughout the carbon cycle. Since the 1990s, ^{14}C has again become useful for detecting fossil fuel CO_2 and is now the principle method for evaluating emissions of fossil fuel CO_2 in atmospheric measurements. For example, patterns of fossil fuel CO_2 hotspots have been observed across much of the world using measurements of atmospheric ^{14}C taken directly in the air and in plant material [7, 8].

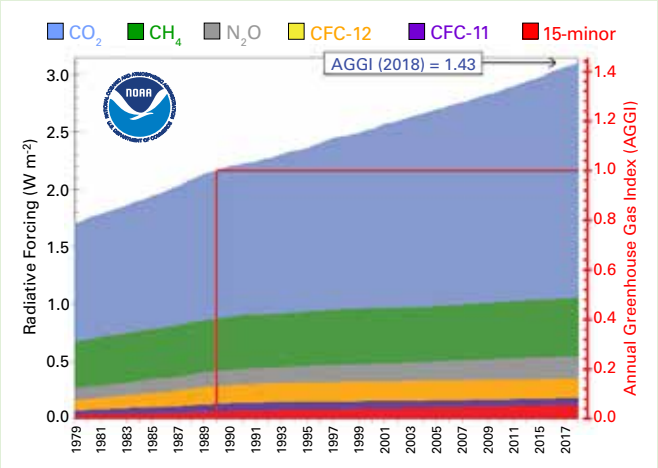

Figure 1. Atmospheric radiative forcing, relative to 1750, of LLGHGs, and the 2018 update of the NOAA AGGI [9].

Table 1. Global annual surface mean abundances (2018) and trends of key greenhouse gases from the GAW global GHG monitoring network. Units are dry-air mole fractions, and uncertainties are 68% confidence limits [12]. The averaging method is described in the GAW Report No. 184 [11]. A number of stations are used for the analyses: 129 for CO_2, 127 for CH_4 and 96 for N_2O.

	CO_2	CH_4	N_2O
2018 global mean abundance	407.8±0.1 ppm	1869±2 ppb	331.1±0.1 ppb
2018 abundance relative to year 1750*	147%	259%	123%
2017–2018 absolute increase	2.3 ppm	10 ppb	1.2 ppb
2017–2018 relative increase	0.57%	0.54%	0.36%
Mean annual absolute increase over the last 10 years	2.26 ppm yr^{-1}	7.1 ppb yr^{-1}	0.95 ppb yr^{-1}

* Assuming a pre-industrial mole fraction of 278 ppm for CO_2, 722 ppb for CH_4 and 270 ppb for N_2O.

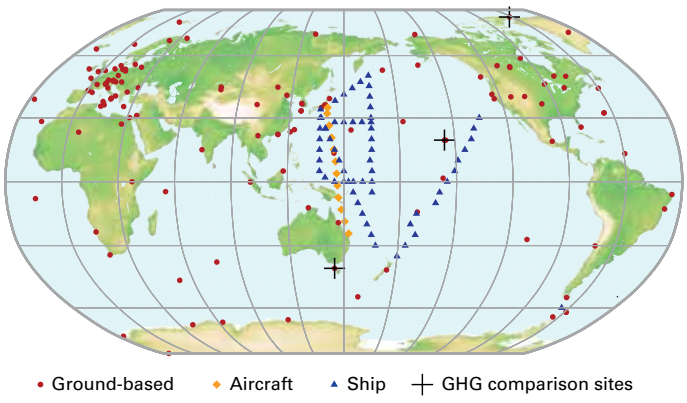

Figure 2. The GAW global network for CO_2 in the last decade. The network for CH_4 is similar.

Executive summary

The latest analysis of observations from the WMO GAW Programme shows that globally averaged surface mole fractions(1) calculated from this in-situ network for carbon dioxide (CO_2), methane (CH_4) and nitrous oxide (N_2O) reached new highs in 2018, with CO_2 at 407.8±0.1 ppm(2), CH_4 at 1869±2 ppb(3) and N_2O at 331.1±0.1 ppb. These values represent, respectively, 147%, 259% and 123% of pre-industrial (before 1750) levels. The increase in CO_2 from 2017 to 2018 was very close to that observed from 2016 to 2017, and practically equal to the average yearly increase over the last decade. For CH_4, the increase from 2017 to 2018 was higher than both that observed from 2016 to 2017 and the average over the last decade. For N_2O, the increase from 2017 to 2018 was also higher than that observed from 2016 to 2017 and the average growth rate over the past 10 years. The National Oceanic and Atmospheric Administration (NOAA) Annual Greenhouse Gas Index (AGGI) [9] shows that from 1990 to 2018 radiative forcing by long-lived greenhouse gases (LLGHGs) increased by 43%, with CO_2 accounting for about 80% of this increase.

Overview of the GAW in-situ network observations for 2018

This fifteenth WMO Greenhouse Gas Bulletin reports atmospheric abundances and rates of change of the most important LLGHGs – CO_2, CH_4 and nitrous oxide N_2O – and provides a summary of the contributions of other gases. These three, together with CFC-12 and CFC-11, account for approximately 96%(4) [9] of radiative forcing due to LLGHGs (Figure 1).

The GAW Programme (http://www.wmo.int/gaw) coordinates systematic observations and analyses of greenhouse gases (GHGs) and other trace species. Sites where greenhouse gases have been measured in the last decade are shown in Figure 2. Measurement data are reported by participating countries, and are archived and distributed by the World Data Centre for Greenhouse Gases (WDCGG) at the Japan Meteorological Agency.

The results reported here by WDCGG for the global average and growth rate are slightly different from those reported by NOAA for the same years [10], due to differences in the stations used, in the averaging procedure and a slightly different time period for which the numbers are representative. The World Data Centre for Greenhouse Gases follows the procedure described in detail in the GAW Report No. 184 [11].

Table 1 provides globally averaged atmospheric abundances of the three major LLGHGs in 2018 and changes in their abundances since 2017 and 1750. Data from mobile stations (blue triangles and orange diamonds in Figure 2), with the exception of NOAA sampling in the eastern Pacific, are not used for this global analysis.

The three GHGs shown in Table 1 are closely linked to anthropogenic activities, and interact strongly with the biosphere and the oceans. Predicting the evolution of the atmospheric content of GHGs requires quantitative understanding of their many sources, sinks and chemical transformations in the atmosphere. Observations from GAW provide invaluable insights into the budgets of these and other LLGHGs, and are used to improve emission estimates and evaluate satellite retrievals of LLGHG column averages.

The Integrated Global Greenhouse Gas Information System (IG^{3}IS, ig3is.wmo.int), promoted by WMO, provides further insights into the sources of GHGs on the national and sub-national level.

The NOAA AGGI [9] in 2018 was 1.43, representing a 43% increase in total radiative forcing (4) by all LLGHGs since 1990 and, on this scale, a 1.8% increase from 2017 to 2018 (Figure 1). The total radiative forcing by all LLGHGs in 2018 (3.1 W m^{-2}) corresponds to an equivalent CO_2 mole fraction of 496 ppm [9].

Carbon Dioxide (CO_2)

Carbon dioxide is the single most important anthropogenic GHG in the atmosphere, contributing approximately 66%[4] of the radiative forcing by LLGHGs (total 3.1 W.m^{-2}). It is responsible for about 82%[4] of the increase in radiative forcing over the past decade and about 81% of the increase over the past five years. The pre-industrial level of 278 ppm represented a balance of fluxes among the atmosphere, the oceans and the land biosphere. The globally averaged CO_2 mole fraction in 2018 was 407.8±0.1 ppm (Figure 3). The increase in annual mean from 2017 to 2018, 2.3 ppm, is nearly the same as the increase from 2016 to 2017 and practically equal to the average growth rate for the past decade (2.26 ppm yr^{-1}).

Atmospheric CO_2 thus reached 147% of the pre-industrial level in 2018, primarily because of emissions from combustion of fossil fuels and cement production (the emissions of fossil fuel CO_2 were projected to reach 36.6 ± 2 $GtCO_2$[5] in 2018 [13]), deforestation and other land-use change (5.5 $GtCO_2$.yr^{-1} average for 2009–2018). Of the total emissions from human activities during the period 2009–2018, about 44% accumulated in the atmosphere, 22% in the ocean and 29% on land; the unattributed budget imbalance is 5% [13]. The portion of CO_2 emitted by fossil fuel combustion that remains in the atmosphere (airborne fraction) varies inter-annually due to the high natural variability of CO_2 sinks without a confirmed global trend.

Methane (CH_4)

Methane contributes about 17%[4] of the radiative forcing by LLGHGs. Approximately 40% of methane is emitted into the atmosphere by natural sources (e.g., wetlands and termites) and about 60% comes from anthropogenic sources (e.g., cattle farming, rice agriculture, fossil fuel exploitation, landfills and biomass burning) [14]. Globally averaged CH_4 calculated from in-situ observations reached a new high of 1869 ± 2 ppb in 2018, an increase of 10 ppb with respect to the previous year (Figure 4). This increase is higher than the increase of 7 ppb in the period 2016–2017 and the average annual increase over the past decade. The mean annual increase of CH_4 dropped from approximately 12 ppb yr^{-1} in the late 1980s to near zero during 1999–2006. Atmospheric CH_4 has been increasing since 2007, reaching 259% of the pre-industrial level (~722 ppb) due to increased emissions from anthropogenic sources. Studies using GAW CH_4 measurements indicate that higher CH_4 emissions from wetlands in the tropics and from anthropogenic sources at mid-latitudes of the northern hemisphere are likely causes of this recent increase (see central insert on the supporting isotopic studies).

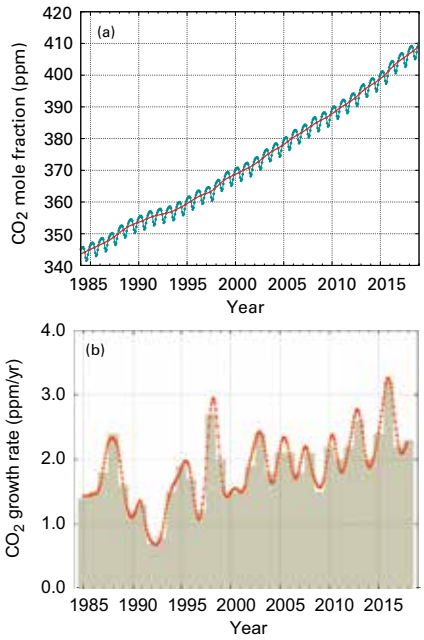

Figure 3. Globally averaged CO_2 mole fraction (a) and its growth rate (b) from 1984 to 2018. Increases in successive annual means are shown as shaded columns in (b). The red line in (a) is the monthly mean with the seasonal variation removed; the blue dots and line depict the monthly averages. Observations from 129 stations have been used for this analysis.

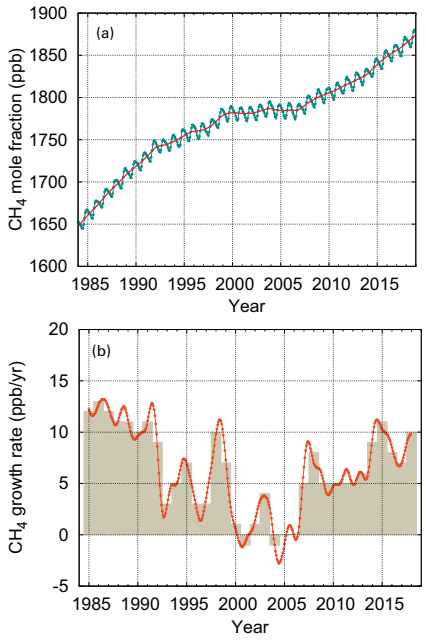

Figure 4. Globally averaged CH_4 mole fraction (a) and its growth rate (b) from 1984 to 2018. Increases in successive annual means are shown as shaded columns in (b). The red line in (a) is the monthly mean with the seasonal variation removed; the blue dots and line depict the monthly averages. Observations from 127 stations have been used for this analysis.

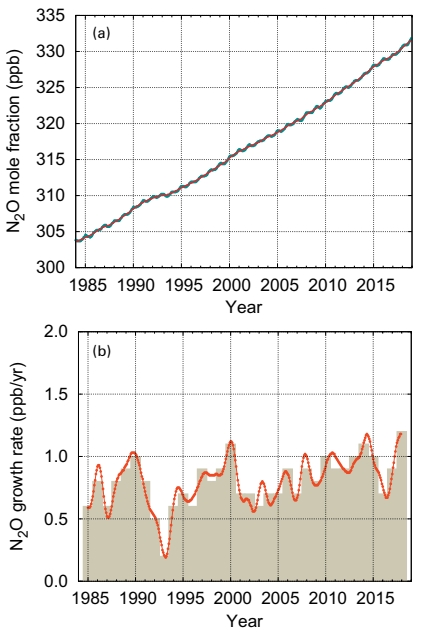

Figure 5. Globally averaged N_2O mole fraction (a) and its growth rate (b) from 1984 to 2018. Increases in successive annual means are shown as shaded columns in (b). The red line in (a) is the monthly mean with the seasonal variation removed; in this plot, it is overlapping with the blue dots and line that depict the monthly averages. Observations from 96 stations have been used for this analysis.

(Continued on page 6)

Use of the stable isotopes to understand changes in global methane levels

Atmospheric methane is the second most important anthropogenic greenhouse gas. It has contributed about 17% of the total radiative forcing by LLGHGs since pre-industrial times, as shown in Figure 6.

As reported in Dlugokencky et al. [18], isotopic measurements carry powerful information about sources of atmospheric methane because they are enriched or depleted in carbon and hydrogen isotopes (^{13}C or D) relative to ambient background air (Figure 7). CH_4 formed at high temperatures (combustion) is enriched in the heavier isotope, and CH_4 from biogenic origin is depleted. Biogenic sources, such as wetlands, have ^{13}C signatures that vary between –70‰ and –60‰ at high northern latitudes, and between –60‰ and –50‰ in tropical climates. Because of different photosynthetic pathways, C3 and C4 plants have very different organic carbon isotope signatures and, when these plants are either burned or digested, the CH_4 released has different isotopic signatures. Therefore, savannah grassland burning (C4) releases CH_4 with $\delta^{13}C$ ranging from –20‰ to –15‰, whereas boreal forest burning releases CH_4 ranging from –30‰ to –25‰. Similarly, ruminants digesting C4 plants give off CH_4 ranging from –55‰ to –50‰, whereas those eating C3 plants give off –65‰ to –60‰ CH_4. The natural gas industry produces CH_4 of variable isotopic signature depending on the formation temperature of the gas reservoir (biogenic or thermogenic). The resultant gas distribution networks contain gas of approximately –50‰ in the Russian pipelines, around –35‰ for the North Sea and in some cases –25‰.

Isotopic measurements can provide some useful insights into the renewed growth of methane that started in 2007. Figure 8 presents in greater detail the recent changes in the global methane level and its ^{13}C content. The changing ratio of carbon isotopes in atmospheric methane, observed since 2007, implies that there has been a significant change in the balance of sources and sinks. In the 1980s, and indeed in the past two centuries, the $\delta^{13}C$-CH_4 trend showed a sustained shift to less negative values (relative increase of ^{13}C) which is indicative of gas leaks and coal emissions [20]. However, the rise observed since 2007 has been accompanied by a decrease in $\delta^{13}C$-CH_4 (relative increase of ^{12}C) [21].

Though there are several hypotheses presented by Nisbet et al. [22], the most plausible is that an increase has occurred in some or all sources of biogenic (wetlands, ruminants or waste) emissions, which contain relatively little ^{13}C. An increase in the proportion of global emissions from microbial sources may have driven both the increase in the methane burden and the shift in $\delta^{13}C$-CH_4.

The other possible explanation is greater emissions from the exploitation of natural gas and oil. This hypothesis would only be consistent with the observed isotopic shift if (a) the new fossil fuel emissions have $\delta^{13}C$-CH_4 markedly more negative than previously thought; (b) there has been a concurrent decline in another source of much more ^{13}C-rich emissions, such as biomass burning; or (c) both changes have occurred. This hypothesis requires more complex investigation.

Atmospheric measurements provide crucial information to solve this complicated puzzle. This remains a key focus of scientific inquiry because $\delta^{13}C$-CH_4 signatures of the different sources are highly variable and sometimes even overlapping (see Figure 7). CH_4 isotope measurements are sparse, and detection of such a small signal is very demanding. New efforts to improve the comparability of international $\delta^{13}C$-CH_4 measurements have recently begun, and greater density of methane isotopic measurements is needed in order to fully understand the drivers of the recent growth in atmospheric methane. To support the technical capabilities of Members to measure isotopic composition, WMO is working with the International Atomic Energy Agency on the technical cooperation project "Developing Capacity towards the Wider Use of Stable Isotopic Techniques for Source Attribution of Greenhouse Gases in the Atmosphere".

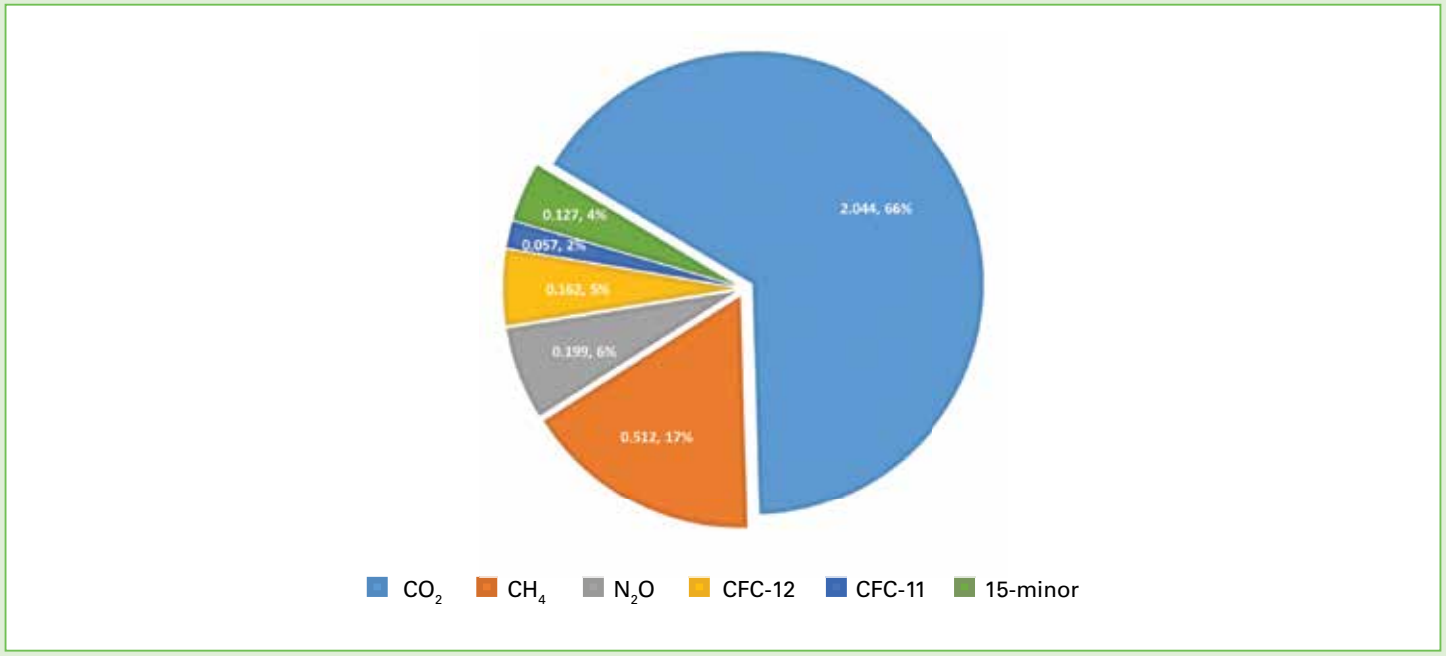

Figure 6. Increase in global radiative forcing in 2018 since pre-industrial times, resulting from an increase atmospheric burden of the most important LLGHGs, expressed in $W.m^{-2}$ and relative to the total increase from all greenhouse gases of 3.1 $W.m^{-2}$ [9].

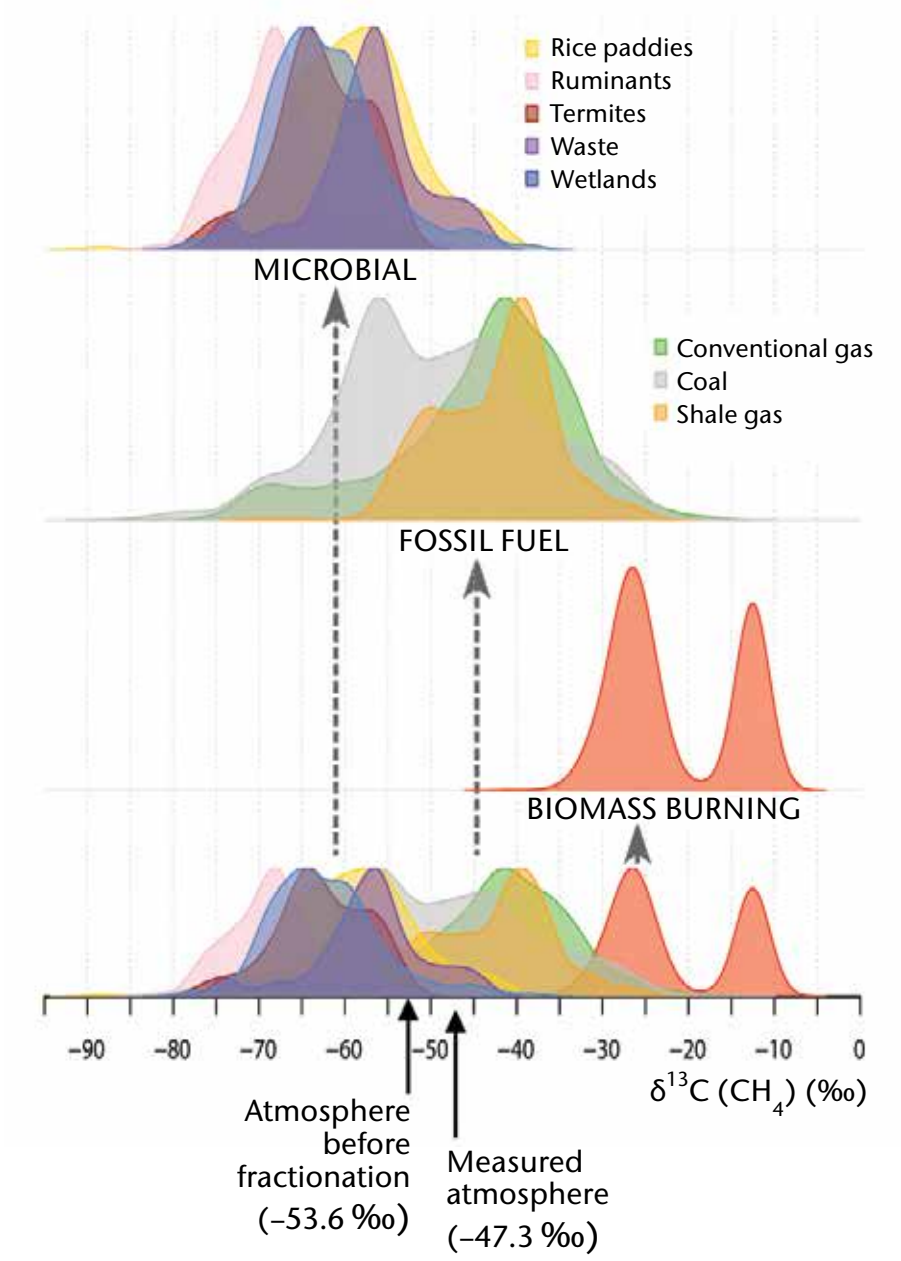

Figure 7. Normalized probability density distributions for the $\delta^{13}C\text{-}CH_4$ of microbial, fossil and biomass burning sources of methane. The flux-weighted average of all sources produces a mean atmospheric $\delta^{13}C\text{-}CH_4$ of approximately −53.6 ‰, as inferred from measured atmospheric $\delta^{13}C\text{-}CH_4$ and isotopic fractionation associated with photochemical methane destruction [19].

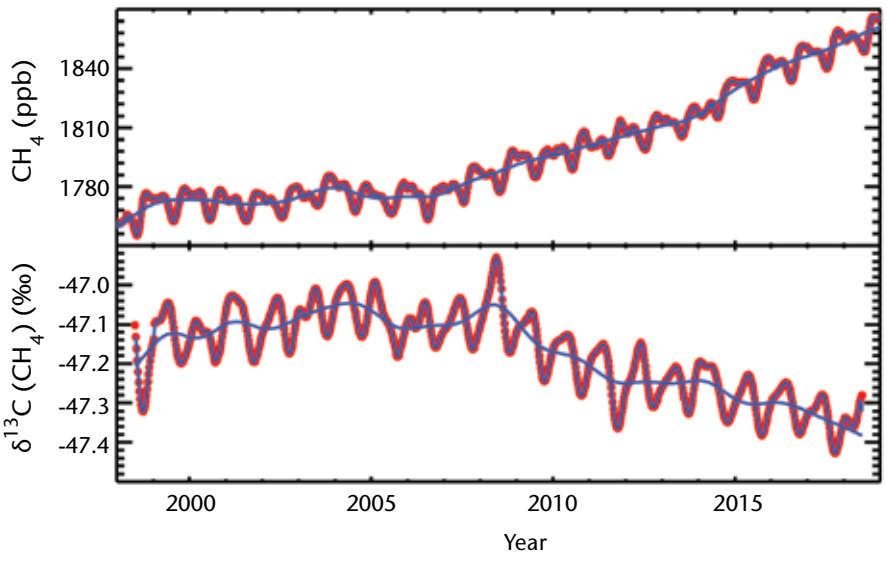

Figure 8. Atmospheric methane at Earth's surface in the remote marine troposphere (from Nisbet et al., 2019 [22]). The upper panel shows globally averaged surface atmospheric CH_4, while the lower panel shows globally averaged surface atmospheric $\delta^{13}C\text{-}CH_4$. The overlapping red and blue lines indicate measurements at weekly resolution, while the single blue line shows the deseasonalized trend (2000–2017). The subset of the global data is from the NOAA network.

Nitrous Oxide (N_2O)

Nitrous oxide contributes about 6%[4] of the radiative forcing by LLGHGs. It is the third most important individual contributor to the combined forcing. N_2O is emitted into the atmosphere from both natural (about 60%) and anthropogenic sources (approximately 40%), including oceans, soils, biomass burning, fertilizer use and various industrial processes. The globally averaged N_2O mole fraction in 2018 reached 331.1 ±0.1 ppb, which is 1.2 ppb above the previous year (Figure 5) and 123% of the pre-industrial level (270 ppb). The annual increase from 2017 to 2018 is higher than the increase from 2016 to 2017 and higher than the mean growth rate over the past 10 years (0.95 ppb yr^{-1}). The likely causes of N_2O increase in the atmosphere are a wider use of fertilizers in agriculture and a higher release of N_2O from soils due to an excess of atmospheric nitrogen deposition related to air pollution [15].

Other greenhouse gases

The stratospheric ozone-depleting chlorofluorocarbons (CFCs), together with minor halogenated gases, contribute approximately 11%[4] of the radiative forcing by LLGHGs. While CFCs and most halons are decreasing, some hydrochlorofluorocarbons (HCFCs) and hydrofluorocarbons (HFCs), which are also potent greenhouse gases, are increasing at relatively rapid rates, even though their abundance is low (at ppt[6] levels). However, at a similarly low abundance, sulphur hexafluoride (SF_6) is an extremely potent LLGHG. It is produced by the chemical industry, mainly as an electrical insulator in power distribution equipment. Its current mole fraction is more than twice the level observed in the mid-1990s (Figure 9a).

This Bulletin primarily addresses LLGHGs. Relatively short-lived tropospheric ozone has a radiative forcing comparable to that of the halocarbons [16]. Many other pollutants, such as carbon monoxide, nitrogen oxides and volatile organic compounds, although not referred to as greenhouse gases, have small direct or indirect effects on radiative forcing. Aerosols (suspended particulate matter) are short-lived substances that alter the radiation budget. All gases mentioned in this Bulletin, as well as aerosols, are monitored by the GAW Programme, with support from WMO Members and contributing networks.

Acknowledgements and links

Fifty-four WMO Members have contributed CO_2 and other GHG data to the GAW WDCGG. Approximately 41% of the measurement records submitted to WDCGG were obtained at sites of the NOAA Earth System Research Laboratory cooperative air-sampling network. For other networks and stations, see GAW Report No. 242 [17]. The Advanced Global Atmospheric Gases Experiment also contributed observations to this Bulletin. Furthermore, the GAW observational stations (Figure 2) that contributed data to this Bulletin are included in the list of contributors on the WDCGG web page (https://gaw.kishou.go.jp/). They also feature in the GAW Station Information System (GAWSIS, https://gawsis.meteoswiss.ch/GAWSIS/) supported by MeteoSwiss, Switzerland.

References

[1] Boden, T.A., R.J. Andres et al., 2017: Global, Regional, and National Fossil-Fuel CO_2 Emissions (1751–2014) (V. 2017). Oak Ridge National Laboratory, Oak Ridge, TN, USA, https://doi.org/10.3334/CDIAC/00001_V2017.

[2] BP, 2019: BP Statistical Review of World Energy, 2019, https://www.bp.com/content/dam/bp/business-sites/en/global/corporate/pdfs/energy-economics/statistical-review/bp-stats-review-2019-full-report.pdf.

[3] Rubino, M., D.M. Etheridge et al., 2019: Revised records of atmospheric trace gases CO_2, CH_4, N_2O, and $\delta^{13}C$-CO_2 over the last 2000 years from Law Dome, Antarctica. *Earth System Science Data*, 11(2), 473–492, doi:10.5194/essd-11-473-2019.

[4] Stuiver, M. and P.D. Quay, 1981: Atmospheric ^{14}C changes resulting from fossil fuel CO_2 release and cosmic ray flux variability. *Earth and Planetary Science Letters*, 53, 349–362.

[5] Levin, I. and V. Hesshaimer, 2000: Radiocarbon: a unique tracer of global carbon cycle dynamics. *Radiocarbon*, 42(1), 69-80.

[6] Turnbull, J.C., S.E. Mikaloff Fletcher et al., 2017: Sixty years of radiocarbon dioxide measurements at Wellington, New Zealand: 1954–2014. *Atmospheric Chemistry and Physics*, 17(23), 14771–14784, https://www.atmos-chem-phys.net/17/14771/2017/.

[7] Shibata, S., E. Kawano and T. Nakabayashi, 2005: Atmospheric [^{14}C]CO_2 variations in Japan during 1982–1999 based on ^{14}C measurements of rice grains. *Applied Radiation and Isotopes*, 63(2), 285–290, https://www.sciencedirect.com/science/article/abs/pii/S096980430500117X.

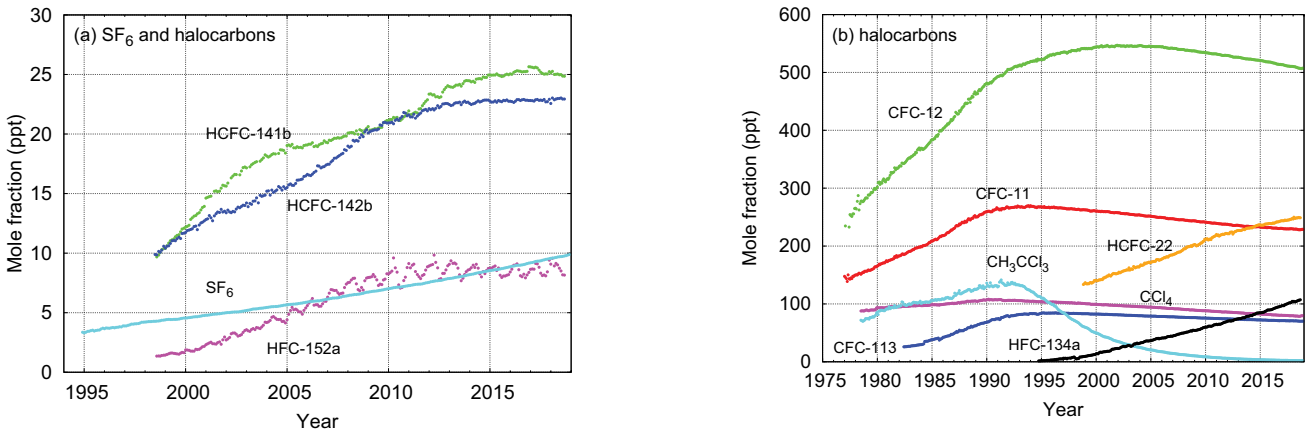

Figure 9. Monthly mean mole fractions of SF_6 and the most important halocarbons: (a) SF_6 and lower mole fractions of halocarbons, and (b) higher halocarbon mole fractions. A number of stations are used for the analyses: SF_6 (85), CFC-11 (23), CFC-12 (25), CFC-113 (21), CCl_4 (22), CH_3CCl_3 (24), HCFC-141b (9), HCFC-142b (14), HCFC-22 (13), HFC-134a (10), HFC-152a (9).

[8] Hsueh, D.Y., N.Y. Krakauer et al., 2007: Regional patterns of radiocarbon and fossil fuel-derived CO_2 in surface air across North America. *Geophysical Research Letters*, 34(2), L02816, https://agupubs.onlinelibrary.wiley.com/doi/10.1029/2006GL027032.
[9] Butler, J.H. and S.A. Montzka, 2019: The NOAA Annual Greenhouse Gas Index (AGGI), http://www.esrl.noaa.gov/gmd/aggi/aggi.html.
[10] National Oceanic and Atmospheric Administration, Earth System Research Laboratory, 2019: Trends in atmospheric carbon dioxide, http://www.esrl.noaa.gov/gmd/ccgg/trends/.
[11] World Meteorological Organization, 2009: Technical Report of Global Analysis Method for Major Greenhouse Gases by the World Data Center for Greenhouse Gases (Y. Tsutsumi, K. Mori, T. Hirahara, M. Ikegami and T.J.Conway). GAW Report No. 184 (WMO/TD-No. 1473), Geneva, https://www.wmo.int/pages/prog/arep/gaw/documents/TD_1473_GAW184_web.pdf.
[12] Conway, T.J., P.P. Tans et al., 1994: Evidence for interannual variability of the carbon cycle from the National Oceanic and Atmospheric Administration/Climate Monitoring and Diagnostics Laboratory Global Air Sampling Network. *Journal of Geophysical Research*, 99:22831–22855, doi:10.1029/94JD01951.
[13] Friedlingstein, P., M.W. Jones et al., 2019: Global Carbon Budget 2019, *Earth System Science Data*, https://doi.org/10.5194/essd-2019-183.
[14] Saunois, M., A.R. Stavert, B. Poulter et al, 2019: The Global Methane Budget 2000–2017, *Earth System Science Data*, https://doi.org/10.5194/essd-2019-128.
[15] Sutton M.A., A. Bleeker, C.M. Howard et al., 2013: Our Nutrient World: The challenge to produce more food and energy with less pollution. Edinburgh, UK, Centre for Ecology and Hydrology, http://www.inms.international/sites/inms.international/files/ONW.pdf.
[16] World Meteorological Organization, 2018: WMO Reactive Gases Bulletin: Highlights from the Global Atmosphere Watch Programme, No. 2, https://library.wmo.int/doc_num.php?explnum_id=5244.
[17] World Meteorological Organization, 2018: 19th WMO/IAEA Meeting on Carbon Dioxide, Other Greenhouse Gases and Related Measurement Techniques (GGMT-2017). GAW Report No. 242, https://library.wmo.int/doc_num.php?explnum_id=5456.
[18] Dlugokencky, E.J., E.G. Nisbet et al., 2011: Global atmospheric methane in 2010: Budget, changes and dangers. *Philosophical Transactions of the Royal Society*, 369, 2058–2072. https://doi.org/10.1098/rsta.2010.0341.
[19] Sherwood, O.A., S. Schwietzke et al., 2017: Global Inventory of Gas Geochemistry Data from Fossil Fuel, Microbial and Burning Sources, version 2017. *Earth System Science Data*, 9, 639–656, https://doi.org/10.5194/essd-9-639-2017.
[20] Rice, A.L., C.L. Butenhoff et al., 2016: Atmospheric methane isotopic record favors fossil sources flat in 1980s and 1990s with recent increase. Proceedings of the National Academy of Sciences of the United States of America, 113, 10791–10796, https://doi.org/10.1073/pnas.1522923113.
[21] Nisbet, E.G., E.J. Dlugokencky. et al., 2016: Rising atmospheric methane: 2007–2014 growth and isotopic shift. *Global Biogeochemical Cycles*, 30, 1356–1370, https://doi.org/10.1002/2016GB005406.
[22] Nisbet, E.G., M.R. Manning et al., 2019: Very strong atmospheric methane growth in the 4 years 2014–2017: Implications for the Paris Agreement. *Global Biogeochemical Cycles*, 33, 318–342, https://doi.org/10.1029/2018GB006009.

Contacts

World Meteorological Organization
Atmospheric Environment Research Division,
Research Department, Geneva
Email: gaw@wmo.int
Website: http://www.wmo.int/gaw

World Data Centre for Greenhouse Gases
Japan Meteorological Agency, Tokyo
Email: wdcgg@met.kishou.go.jp
Website: https://gaw.kishou.go.jp/

Notes:

(1) Mole fraction= the preferred expression for abundance (concentration) of a mixture of gases or fluids. In atmospheric chemistry it is used to express the concentration as the number of moles of a compound per mole of dry air

(2) ppm = number of molecules of the gas per million (10^6) molecules of dry air

(3) ppb = number of molecules of the gas per billion (10^9) molecules of dry air

(4) This percentage is calculated as the relative contribution of the mentioned gas(es) to the increase in global radiative forcing caused by all long-lived greenhouse gases since 1750.

(5) 1 $GtCO_2$ = 1 billion (10^9) metric tons of carbon dioxide

(6) ppt = number of molecules of the gas per trillion (10^{12}) molecules of dry air

Selected greenhouse gas observatories

Park Falls, Wisconsin (LEF)

The atmospheric monitoring station located at the LEF TV transmitter tower in Park Falls, Wisconsin, USA (45.9451° N, 90.2732° W, 472 m a.s.l.) is operated by NOAA in collaboration with the Wisconsin Educational Communications Board, the US Geological Survey and the University of Wisconsin. The 447 m-tall TV transmitter tower has served as a platform for making reference quality atmospheric CO_2 measurements for 25 years (operation began in October 1994) and now hosts a suite of complementary measurements including in-situ measurement of CH_4 and CO, daily discrete air samples that are measured for more than 50 compounds at central facilities in Boulder, and observations of CO_2 in the total column of the Earth's atmosphere. Tall towers such as LEF are ideal measurement platforms for monitoring greenhouse gases at continental sites. Inlets at multiple levels on the tower (30 m, 122 m and 396 m above ground level in the case of LEF) allow for observations of CO_2 vertical gradients in the boundary layer that can be used to distinguish local and remote sources and sinks. The top inlet level on the LEF tower routinely sees air representative of large areas of continental United States and Canada, and provides information on regional processes at a continental location. These measurements provide valuable insights into regional processes in global models.

Amazon aircraft programme

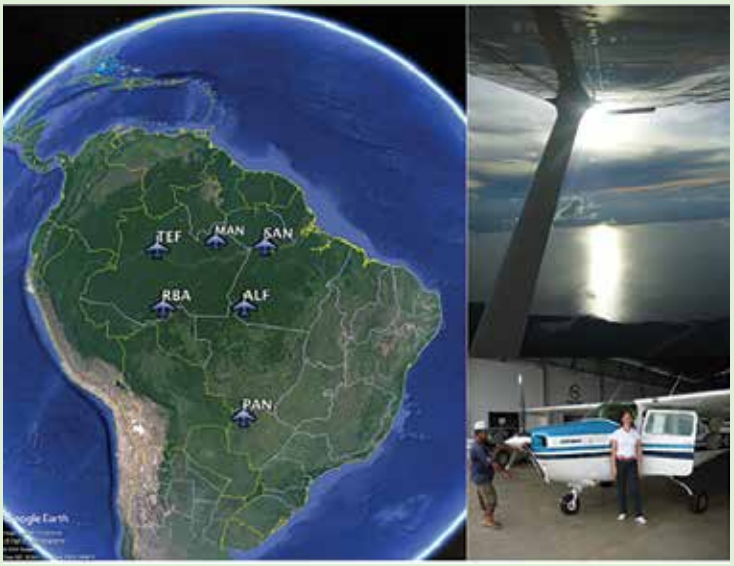

The Earth System Science Center of the National Institute for Space Research (INPE), São José dos Campos, Brazil, has made vertical profile measurements of CO_2, CH_4, N_2O, SF_6 and CO over the Brazilian Amazon since 2004. The Brazilian vertical profile network uses small commercial aircraft to collect discrete air samples at multiple altitudes (0.3 km–7 km) over sites in Brazil, at bi-weekly to monthly intervals. The sites are chosen so that they allow for monitoring of changes in GHG abundance, as air traverses the Brazilian Amazon, and for mass balance studies of Amazonian fluxes. Currently, there are six active sites: Santarém (2.86° S, 54.95° W), Manaus (2.60° S, 60.21° W), Rio Branco (9.38° S, 67.62° W), Alta Floresta (8.80° S, 56.75° W), Tefé (3.39° S, 65.6° W) and Pantanal (19.49° S, 56.38° W). To date, over 860 vertical profiles have been taken. They provide important information on the response of the Amazon to climate change and supply critical verification data for satellite retrievals in tropical regions.

JN 191536